

Research on the Output Performance of a Solar-Cooled PV/T System

Yaolin Zhu¹, Hanning Zhu², Yongfeng Zhu³

¹Third Middle School, Selibuya Town, Kashgar 844000, Xinjiang, China

²College of Chemistry and Chemical Engineering, Changji University, Changji 831100, Xinjiang, China

³Shizong Dalaisheng Biotechnology Co., Ltd., Qujing 655000, Yunnan, China

Copyright: © 2025 Author(s). This is an open-access article distributed under the terms of the Creative Commons Attribution License (CC BY 4.0), permitting distribution and reproduction in any medium, provided the original work is cited.

Abstract: Owing to their high practicability, solar PV/T (photovoltaic/thermal) collectors have attracted considerable attention from researchers in both photovoltaic and solar-thermal fields worldwide. In this study, we designed and constructed a novel solar-cooled PV/T system. Through experimental methods, we conducted an in-depth investigation of its thermal and electrical output characteristics and developed mathematical models for both thermal performance and electrical performance. Finally, we validated the experimental data against simulations. The results demonstrate that the designed solar-cooled PV/T system exhibits excellent thermal and electrical output performance. The utilization rate of waste heat from the PV module's back plate reached 18.59%, and the system's electrical efficiency improved by 1.92% compared to a conventional PV/T system. This work provides theoretical and experimental guidance for the further optimization and improvement of the solar-cooled PV/T system.

Keywords: PV/T systems; Solar energy; Output performance

Online publication: 29 May, 2025

1. Introduction

In recent years, awareness of the energy crisis, financial instability, and climate change has grown markedly, sparking a global surge in research on new energy sources and their utilization ^[1]. Solar PV module power generation is highly dependent on operating temperature: studies have shown that each 1°C rise in the back-plate temperature of a PV module reduces its output power by 0.4–0.5%. More than 80% of the solar irradiance incident on a PV module surface is converted into heat, causing module temperatures to often exceed 50°C, whereas the optimal back-plate temperature for photovoltaic conversion is around 45°C. Under poor cooling conditions, temperatures can rise above 90°C, severely degrading PV efficiency ^[2]. By combining photovoltaic cells with a thermal collector, a PV/T collector is formed. In such a system, a working fluid (typically water) circulates behind the PV module, removing excess heat so that the module operates near its optimal temperature while simultaneously generating thermal energy. This dual extraction of electricity and heat greatly enhances overall

solar energy utilization efficiency.

The prospects and value of solar PV/T systems are widely recognized. Leading scholars predict that PV/T technology will undergo growth trends similar to those seen in standalone photovoltaic and solar-thermal technologies. Numerous researchers have investigated various PV/T configurations and their performance. Dai and He designed a solar PV/T-absorption heat-pump water-heating system^[3]. After the heat-pump cycle, the insulated storage tank's temperature rose by approximately 30 °C, enabling the system to be self-sustaining. He *et al.* developed a concentrating PV/T water-heating system^[4]. By analyzing the system's energy-conversion efficiency, storage capability, and energy-transfer characteristics alongside electrical and thermal output data, they showed that this PV/T system could meet the low-power electricity and hot-water needs of rural households, demonstrating practical value. Xu conducted a rooftop PV/T performance analysis based on mathematical modeling^[5], exploring the interactions and constraints among system components, establishing a simulation model, and designing a simulation workflow for solution finding. Foreign scholar Shmelev *et al.* demonstrated that a hybrid PV/T solar system can simultaneously supply electricity and heat^[6], achieving higher solar-radiation conversion rates than standard PV modules. They proposed that, with proper design, PV/T systems can extract heat from PV modules to heat water or air—thereby lowering module operating temperatures and maintaining high electrical efficiency. Their research confirmed that PV/T systems can generate substantial amounts of both heat and electricity, offering economic feasibility.

In a comparative study on compound cooling modes for PV/T modules, Du *et al.* founded that increasing both air and water mass flow rates enhances the PV/T module's combined electrical–thermal performance^[7], achieving a maximum overall efficiency of 84.46%. In the compound cooling mode, temperature stratification on the glass cover was evident, and electrical efficiency increased by 16.09% compared to modules without fluid cooling. Dong *et al.* reviewed advances in PV/T technology^[8], noting that many challenges remain, particularly in analyzing long-term dynamic performance. Razali *et al.* experimentally tested a PV/T collector and demonstrated that both thermal and electrical efficiencies increase with higher mass flow rates^[9]. Khanjari *et al.* used numerical simulations to study the impact of nanofluids on PV/T performance^[10], finding that nanofluids enhance the working fluid's thermal-physical properties and accelerate heat exchange. Nasrin *et al.* introduced a novel PV/T system employing nanofluids and reported an overall efficiency of approximately 89% through combined experimental and numerical analysis^[11]. In summary, further structural optimization and the development of new PV/T collectors are needed.

Accordingly, this paper presents the design of a solar-cooled PV/T power and hot-water system. We mounted absorber tubes, fins, collector plates, and insulation materials behind the PV modules and installed a full-glass vacuum tube collector on one side. The heat generated by the PV modules transfers to the heat-transfer fluid in the absorber tubes, stabilizing the PV module temperature and preventing efficiency loss from overheating. The preheated fluid then flows to the external collector for further heating, and the reheated fluid is stored. We investigate system output performance—including electrical characteristics, thermal characteristics, and overall energy efficiency—across five sections: an introduction outlining the research background and objectives; the design and construction of the solar-cooled PV/T system; development of theoretical mathematical models; data acquisition and model validation; and, finally, conclusions.

2. Design and construction of the solar-cooled PV/T system

2.1. Current challenges in photovoltaic power generation technology

Photovoltaic (PV) power generation relies on the photoelectric effect in semiconductor materials: when light strikes a p–n junction, it directly converts photons into electric power. A typical PV power system comprises four main components: PV modules, a charge controller, an inverter, and an energy storage device. Although national policies strongly support photovoltaic power generation, the technology has several drawbacks. First, its photoelectric conversion efficiency remains relatively low—today’s crystalline silicon modules achieve only about 12–21% efficiency, while amorphous silicon modules reach just 6–8%^[12]. Second, PV systems generate electricity only when exposed to sunlight, producing no power at night, which limits compatibility with everyday energy consumption patterns. Third, PV output is highly susceptible to weather: extended overcast, rainy, snowy, or foggy conditions, as well as rapid cloud movements, all degrade generation efficiency. Fourth, PV performance depends strongly on geographic location—differences in local solar irradiance mean generation varies widely from region to region. Finally, although the Sun’s total incident energy on Earth is enormous, less than 10% actually reaches the land surface (most is absorbed or reflected by oceans and the atmosphere), resulting in a low energy density at ground level. Additional limitations include large land requirements, high system costs, and the energy- and pollution-intensive manufacturing process of crystalline silicon cells; module performance also deteriorates at elevated operating temperatures.

2.2. Structure of the solar-cooled PV/T system

Over the past four decades, researchers have found that excessive back-plate temperatures in PV modules sharply reduce their electrical efficiency. This insight gave rise to PV/T (photovoltaic/thermal) research, since PV/T systems combine the strengths of standalone PV and solar-thermal collectors and attract considerable attention for their dual-generation capabilities. Advances in phase-change materials (PCM) and nanofluids have accelerated PV/T development, with most improvements focusing on thermal management rather than electrical optimization. Reviews of earlier studies indicate that PV/T collectors hold great promise for preheating air in future applications^[13].

The solar-cooled PV/T system employs a circulating water loop behind the PV modules to transfer heat away from the back plate, thereby reducing module temperature and enhancing electrical efficiency. Our system consists of the following key components: copper absorber tubes for the circulation loop; aluminum-foil absorber plates; high-density polyurethane insulation with foil lining; full-glass vacuum tubes; PV modules; a battery bank; a PV charge controller; and auxiliary electrical loads (e.g., 18 W energy-saving lamps). **Figure 1** shows photographs of these components: (a) PV module back plate lined with foil, (b) PV/T aluminum-foil absorber plate, (c) PV/T PV module, (d) cooling circulation loop, (e) solar irradiance meter, (f) PV/T battery storage system, (g) makeup water tank, and (h) system controller. Thermal performance data are collected using a TCM-2Z solar thermal performance tester. Electrical performance measurements and analyses employ a digital ammeter, a digital voltmeter, an AC/DC digital multimeter, and a solar-simulator PV test bench.

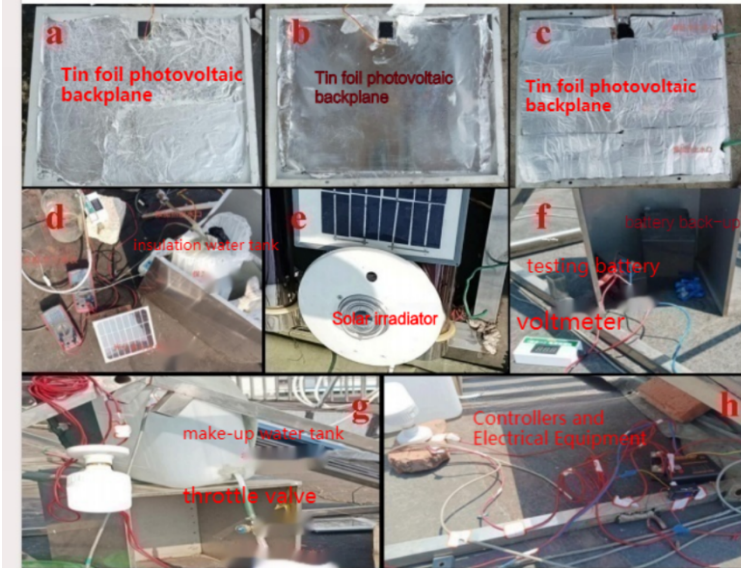


Figure 1. Photograph of the main components of the system

2.3. Fundamental parameters of the solar-cooled PV/T system

2.3.1. Thermal performance parameters

Figure 2 shows the physical setup of the solar-cooled PV/T system. Thermal performance data are collected using a TCM-2Z solar thermal performance tester. Channels 1–25 serve as temperature-probe inputs; channels 26–27 measure ambient temperature; channel 28 measures wind speed (ignored in this study); channel 30 connects to the solar irradiance meter; and channel 32 interfaces with the computer for data acquisition.



Figure 2. Physical setup of the solar-cooled PV/T system

To characterize thermal output, we record the inlet and outlet temperatures of the full-glass vacuum tube collector. In addition, real-time temperatures at the upper, middle, and lower positions of a standby tube are monitored. Solar irradiance is measured via the irradiance meter connected to channel 30 of the TCM-2Z tester. Ambient temperature is logged continuously via channels 26 and 27; because Chuxiong’s hot, humid climate can introduce measurement error, we cross-validate the tester’s ambient readings with an independent digital temperature sensor. Back-plate temperature of the PV modules (control group), inlet temperature to the circulation loop, and pre-heated water temperature in the insulated tank are all measured with the TCM-2Z.

2.3.2. Electrical performance parameters

Electrical measurements include open-circuit voltage, short-circuit current, ambient temperature, initial battery voltage, and the I–V characteristic curve of the PV modules under standard conditions. The PV modules (observing polarity), load (an 18 W LED lamp), and battery are all connected through the PV charge controller. Ambient temperature is measured via a standalone digital temperature sensor, which is used to calibrate the tester’s probe. A digital voltmeter, digital ammeter, and AC/DC multimeter record the system’s electrical performance parameters. The I–V curve is obtained using a dedicated PV performance analyzer under a solar simulator.

2.4. Overall energy efficiency parameters

Figure 3 presents a schematic diagram of the solar-cooled PV/T system’s operation. Total system efficiency is determined by integrating the measured solar irradiance over time to compute the total incident energy, then applying calculus-based mathematical models to calculate energy inputs and outputs. Experimental results are used to validate the model.

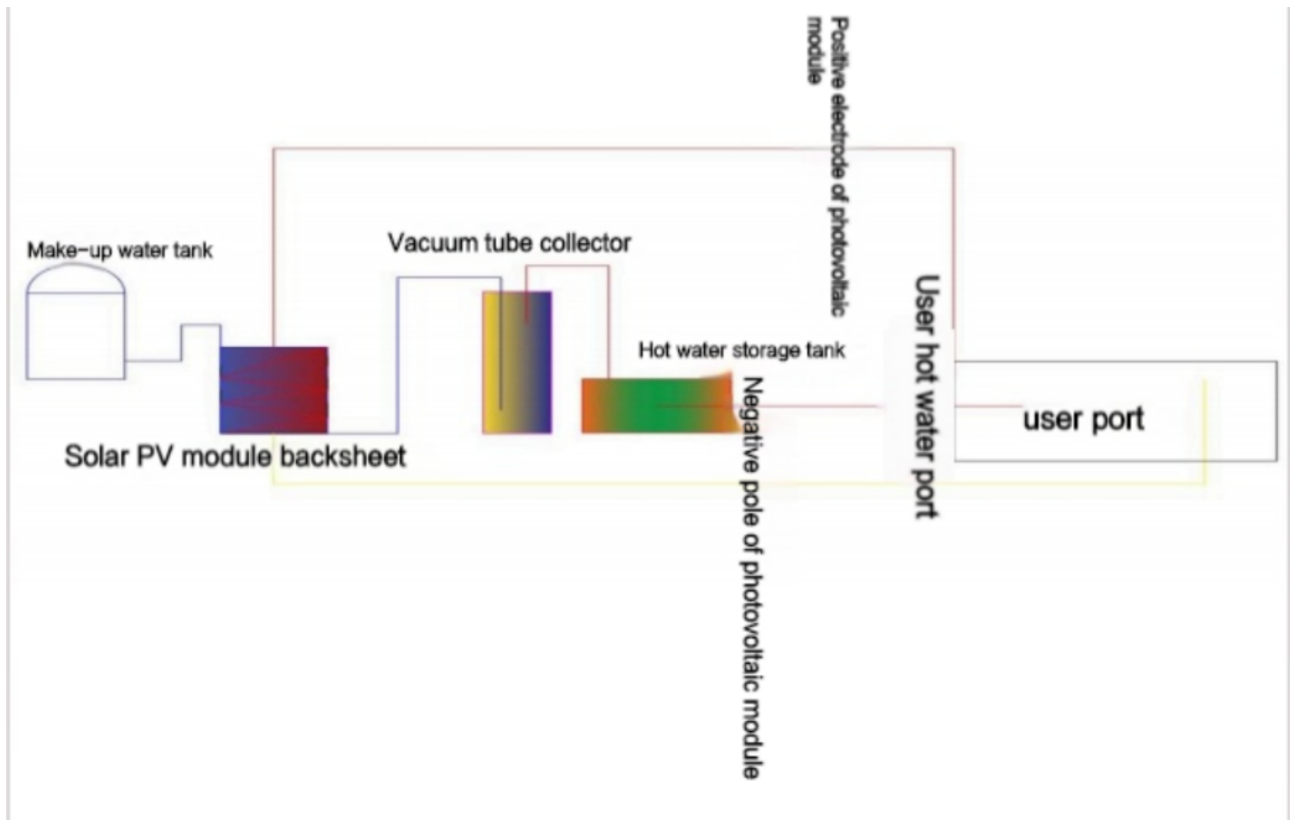


Figure 3. Operational schematic of the solar-cooled PV/T system

3. Design and establishment of the thermal performance model for the solar-cooled PV/T system

3.1. Establishment of the thermal performance model

3.1.1. Thermal performance of the full-glass vacuum tube

The calculation of solar thermal utilization begins by determining the solar declination angle δ , which is the angle between the line connecting the centers of the Earth and Sun and the plane of the Earth's equator. Since our model does not specifically target equinoxes or solstices, we use the declination formula from Zhang's Principles of Solar Thermal Utilization and Computer Simulation^[14]:

$$\delta = 23.45 \sin \left(360^\circ \times \frac{284+n}{365} \right) \quad (1)$$

where n is the day number of the year (January 1 = 1, using the Gregorian calendar).

To ensure accurate insolation calculations, we must also match the model to the local sunrise and sunset times on the test day:

$$\cos \omega = -\tan \delta \tan \phi \quad (2)$$

where ϕ is the local latitude in degrees and ω is the hour angle at sunrise or sunset in degrees. Continuing this derivation yields:

$$\omega = \cos^{-1} (-\tan \delta \tan \phi) \quad (3)$$

From which we can compute the sunrise and sunset times via:

$$N = \frac{2\omega}{15} = \frac{2}{15} \cos^{-1} (-\tan \delta \tan \phi) \quad (4)$$

Here we adopt the solar noon at Chuxiong Normal University as 13:15 local time for simplicity.

Next, the instantaneous solar irradiance on a tilted surface at the test site is given by:

$$G_0 = G_{sc} \left[1 + 0.033 \cos \left(\frac{360^\circ n}{365} \right) \right] \cos \theta \quad (5)$$

where G_0 is the irradiance in W/m^2 , θ is the collector tilt angle in degrees, and G_{sc} is the solar constant ($1353 W/m^2$).

Integrating over a full day yields the daily irradiation H_0 :

$$H_0 = \frac{24 \times 3600 G_s}{\pi} \left[1 + 0.033 \cos \left(\frac{360^\circ n}{365} \right) \right] \times \left[\cos \phi \cos \delta \sin \omega + \frac{2\pi\omega}{360^\circ} \sin \phi \sin \delta \right] \quad (6)$$

where H_0 is in J/m^2 . The irradiation over any hour, I_0 , is then

$$I_0 = \frac{24 \times 3600 G_s}{\pi} \left[1 + 0.033 \cos \left(\frac{360^\circ n}{365} \right) \right] \times \left[\sin \omega_2 - \sin \omega_1 + \frac{2\pi(\omega_2 - \omega_1)}{360^\circ} \sin \phi \sin \delta \right] \quad (7)$$

where ω_1 and ω_2 are the hour angles at the beginning and end of the interval (in degrees), with $\omega_2 > \omega_1$. Because the site lies in the Northern Hemisphere and faces due south (azimuth $\gamma = 0^\circ$) to maximize insolation, we apply a radiation correction factor $R = 0.1343$.

Finally, the effective collector area of the cooled PV/T system is

$$A = 2r \times 1.8 \times a \quad (8)$$

where r is the outer diameter of the vacuum tube ($GB = 47 \times 10^{-2} m$) and a is the number of tubes.

3.2. Establishment of the electrical performance model for the solar-cooled PV/T system

3.2.1. Conversion efficiency of the PV modules

To model the electrical efficiency of the solar-cooled PV/T system, we begin with the open-circuit voltage, denoted U_{oc} (in volts), which is the voltage across the V module when no load is connected and the module is illuminated.

A key parameter in photovoltaic performance is the fill factor, FF, defined as the ratio of the actual maximum power output of the PV module to the product of its open-circuit voltage and short-circuit current ^[15]:

$$FF = \frac{P_m}{U_{oc}I_s} = \frac{U_m I_m}{U_{oc}I_s} \quad (9)$$

Among them, U_m represents the maximum voltage of the photovoltaic module, with the unit being volts; I_m indicates the maximum current of the photovoltaic module, with the unit being amperes; P_m represents the maximum output power of photovoltaic modules, with the unit being watts.

$$\eta = \frac{FF \times U_{oc} \times I_s}{G \times A_g} \times 100\% \quad (10)$$

3.2.2. Energy yield of the PV modules

Calculate using the following formula:

$$E_p = H_A \times \frac{P_{AZ}}{E_S} \times K \quad (11)$$

In Formula (11), where H_A is the total solar irradiation on the test plane ($\text{kW} \cdot \text{h}/\text{m}^2$), E_S is the standard-test-condition irradiance (kW/m^2), P_{AZ} is the theoretical rated power of the PV array (W), and K is the overall system performance coefficient (typically 0.9).

3.3. Establishment of the overall energy efficiency model

3.3.1. Total input energy

The total energy received by the system is derived from solar radiation energy and is calculated using Equation 12:

$$G_Z = \int_{t_1}^{t_2} AG \cdot d_T \quad (12)$$

Where G_Z is the total solar irradiance energy, with the unit W (watt), and t_1 is the initial time at the time of calculation.

3.3.2. Total output energy

The total output energy comprises the electrical energy generated by the PV modules during peak-sun hours plus the thermal energy captured and converted by the solar collector.

3.3.3. Overall system efficiency

The total energy efficiency of the system is calculated using the following formula:

$$\eta_Z = \frac{W_{have}}{W_{total}} \quad (13)$$

4. Solar cooling PV/T model data collection and model validation

4.1. Experimental data collection

Heat is collected through a heat collection plate (aluminum foil), and the residual heat from the photovoltaic (PV) module backplate is extracted using a heat collection channel (copper tube). Preheated water in the collector is then transferred to an insulated water tank for temperature testing. The utilization rate is analyzed and compared through theoretical calculations.

Data statistics are performed by calculating the average short-circuit current and open-circuit voltage over the measured time periods. The performance data for conventional PV modules are shown in **Table 1** below:

Table 1. Performance parameters of conventional PV modules

Time period	Current (A)	Voltage (V)	Backplate temperature (°C)	Irradiance (W/m ²)
07:00–11:00	1.28	14.05	37.1	490.09
11:00–15:00	2.62	17.54	48.54	902.52
15:00–19:10	1.00	13.83	39.14	402.26

From **Table 1**, it is evident that experimental data collection was divided into three time periods: morning, noon, and afternoon. The results show that solar irradiance is optimal during the noon period, with the average backplate temperature of the PV modules also being the highest. Without cooling, this high temperature would lead to a reduction in the power generation efficiency of the PV modules.

The performance data for the cooled PV/T system are presented in **Table 2** below:

Table 2. Performance parameters of cooled PV/T modules

Time period	Current (A)	Voltage (V)	Backplate temperature (°C)	Irradiance (W/m ²)
07:00–11:00	1.34	20.80	34.18	513.93
11:00–15:00	2.54	20.11	41.25	1006.40
15:00–19:10	0.96	19.36	36.38	314.09

Table 2 shows the trends in current, voltage, backplate temperature, and solar irradiance for the cooled PV/T modules across different time periods. It is clear that the backplate temperature of the cooled PV/T modules is slightly higher at noon compared to the morning and afternoon periods.

For the all-glass vacuum tube collector, data were collected using three test tubes over a one-week period. The experimental data were divided into three time periods each day, processed using the average value method, and compiled statistically. The following table shows the inlet temperature data for the vacuum collector, with a fixed water volume (4500 mL) and no water replacement or circulation during testing.

From **Table 3**, it can be observed that during thermal performance testing, the inlet water temperature of the all-glass vacuum tube collector satisfies the trend: morning < noon < afternoon.

Table 3. Inlet temperature statistics for the collector

Time period	10th	11th	12th	13th	14th	15th	20th
07:00–11:00	24.67	22.28	24.67	26.14	28.31	25.17	31.24
11:00–15:00	41.13	64.41	62.17	76.39	79.85	75.14	43.75
15:00–19:10	75.46	91.30	83.39	88.89	94.14	93.22	39.97

According to **Table 4**, the outlet temperature of the collector is highest in the afternoon, reaching a maximum of 105.41°C, and lowest in the morning, with a minimum of 29.93°C.

Table 4. Outlet temperature statistics for the collector

Time period	10th	11th	12th	13th	14th	15th	20th
07:00–11:00	48.58	34.23	39.20	40.52	35.09	29.93	47.20
11:00–15:00	62.17	94.71	89.10	85.54	92.69	86.61	64.69
15:00–19:10	83.39	102.67	99.88	90.83	105.41	99.63	53.44

From **Table 5**, it is clear that the temperature of the supply water tank in the cooled PV/T system remains relatively stable, with the noon period's average water temperature being closest to the daily average supply tank temperature.

Table 5. Temperature statistics for the cooled PV/T system supply water tank

Time period	Supply tank temperature (°C)	Average temperature (°C)
07:00–11:00	20.83	25.14
11:00–15:00	25.40	
15:00–19:10	28.48	

From **Table 6**, it can be concluded that during data collection, the circulating water utilizes the residual heat from the PV module backplate as it passes through. The average temperature of the insulated water tank during testing was 36.49°C.

Table 6. Temperature statistics for the cooled PV/T system insulated water tank

Time period	Insulated tank temperature (°C)	Average temperature (°C)
07:00–11:00	25.59	36.49
11:00–15:00	37.77	
15:00–19:10	35.25	

Based on data collected on April 12, 2023, at the Renewable Energy Engineering Training Base on the roof of the Duxue Building at Chuxiong Normal University, a power versus time trend chart was generated for conventional solar PV modules (without a cooling water circulation system), as shown in **Figure 4**.

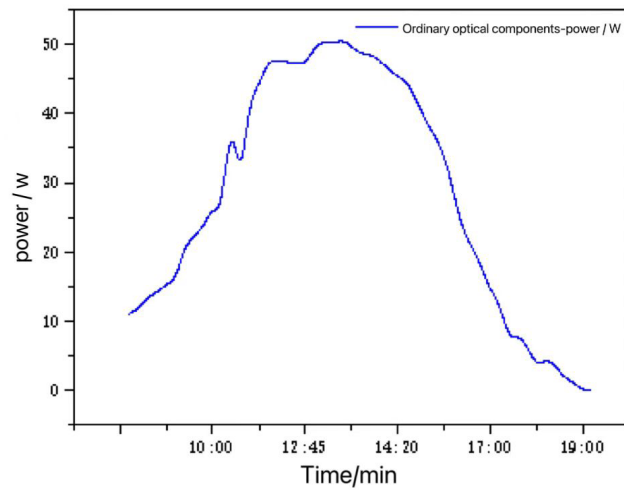


Figure 4. Power of control group PV modules

Using the same statistical methods, performance testing of the cooled PV/T modules was conducted on April 20, 2023. The maximum solar irradiance on that day was 1113 W/m^2 , with a maximum ambient temperature of 31.6°C , a maximum voltage of 20.9 V , and a maximum short-circuit current of 2.71 A . The average backplate temperature of the cooled PV/T system modules was maintained within the standard range at 47.57°C , with specific averages of 31.52°C from 07:30–10:59, 50.15°C from 11:00–14:59, and 41.83°C from 15:00–17:10. A total of 703 data points were collected throughout the day, providing reliable results.

From **Figure 5**, it is evident that the power variation of the cooled PV/T modules is significant, with an average daily power output of 32.69 W .

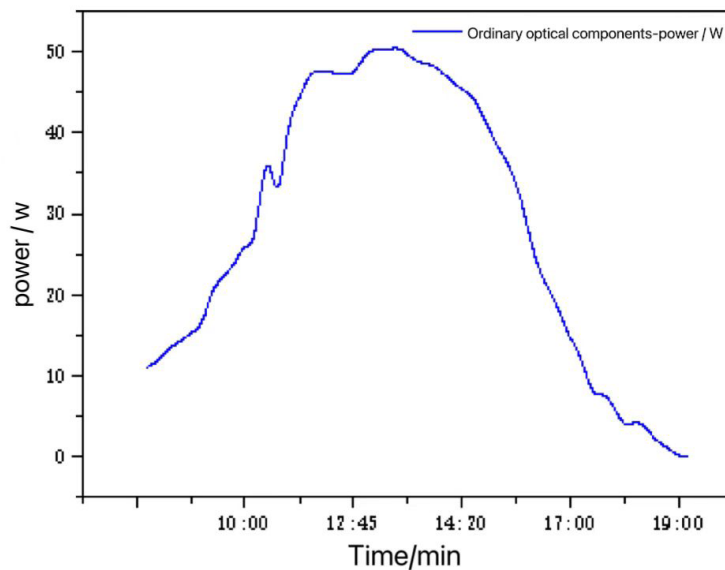


Figure 5. Power of cooled PV/T system PV modules

Figure 6 shows the thermal performance test chart for the all-glass vacuum tube collector, including inlet

and outlet temperatures for Test Tube 1 of the cooled PV/T system, as well as the ambient temperature and solar irradiance on the test day. The upper, middle, and lower temperatures of Test Tube 2 were also measured and recorded.

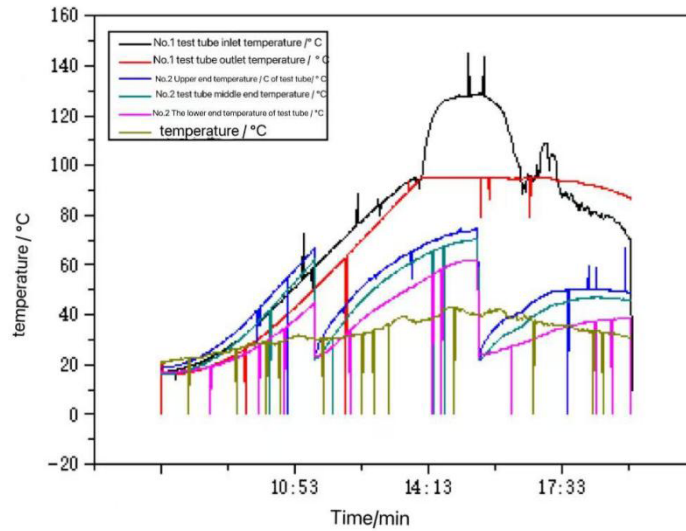


Figure 6. Performance of all-glass vacuum tube collector

Figure 7 shows the solar irradiance on April 15, 2023, during testing of conventional PV modules, with a maximum value of 758 W/m².

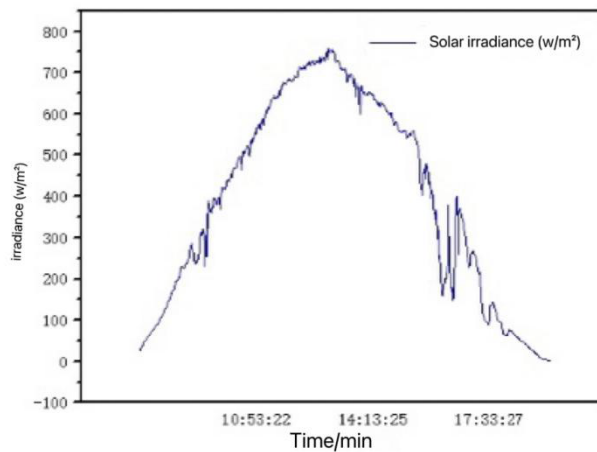


Figure 7. Solar irradiance on April 15, 2023

Figure 8 shows the solar irradiance on April 20, 2023, during testing of the cooled PV/T system modules, with a maximum value of 1113 W/m² at 13:00.

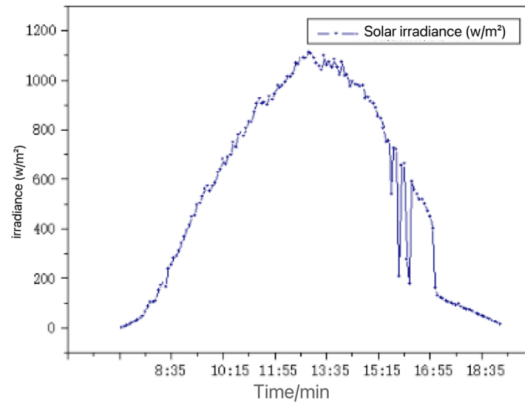


Figure 8. Solar irradiance on April 20, 2023

Figure 9 shows the backplate temperature of the solar PV modules in the cooled PV/T system after cooling with circulating water, with a maximum temperature of 57°C and an average of 42.65°C .

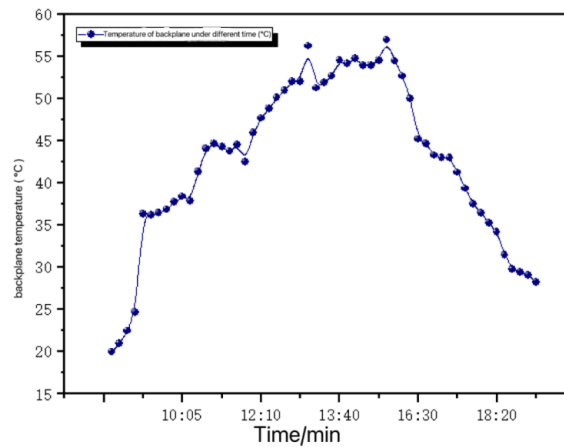


Figure 9. Backplate temperature of cooled PV/T modules

Figure 10 illustrates the backplate temperature of conventional PV modules during electrical performance testing, with a maximum of 95.9°C and an average of 73.97°C .

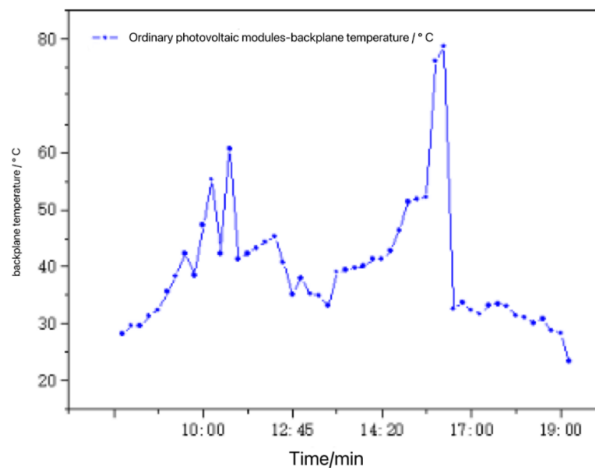


Figure 10. Backplate temperature of conventional PV modules

Figure 11 shows the ambient temperature on the test day, with a maximum of 31.6°C.

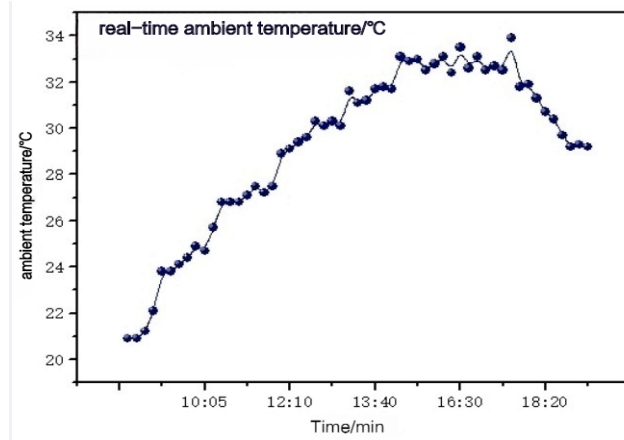


Figure 11. Ambient temperature

Figure 12 shows the temperature of the supply water tank used for circulating cooling water during system testing, with an average daily temperature of 25.14°C.

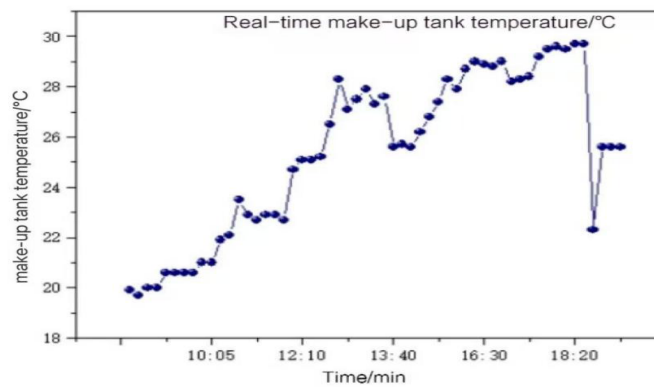


Figure 12. Supply water tank temperature

Figure 13 shows the temperature trend of the circulating water in the PV/T system, with a maximum temperature of 50.7°C and an average daily temperature of 36.49°C.

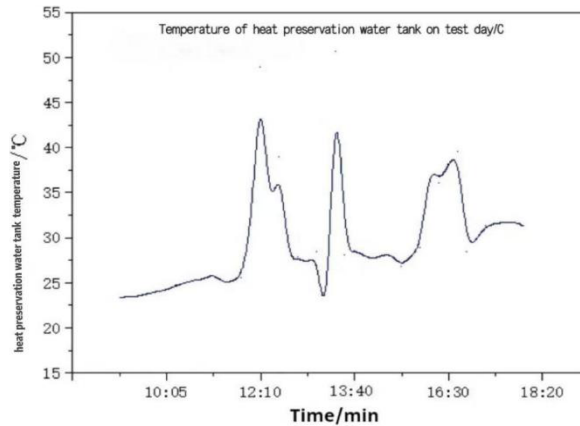


Figure 13. Insulated water tank temperature

4.2. Experimental model data analysis and validation

4.2.1. Thermal performance of the model

Based on Equation (14):

$$Q = \int C_V M dT = 4.2 \times 10^3 \text{ J/kg} \cdot ^\circ\text{C} \times 4.5 \text{ kg} \times (47.2 - 31.24) ^\circ\text{C} = 301.64 \text{ kJ} \quad (14)$$

Where Q is heat required to increase water temperature, in kJ, M is mass of the working medium, in kg, C_v is specific heat capacity of the working medium, in J/(kg·°C).

Using Equations (1) to (7), the solar irradiance absorbed by the vacuum tube collector during the morning period on April 20, 2023, was calculated to be 0.305 MJ. This value is slightly higher than the heat required as per Equation (14), indicating that the collected data for this system are valid.

Using Equation (14), the heat required to raise the water temperature to 64.69°C at noon on April 20 was calculated to be 395.76 kJ. The solar irradiance absorbed by the vacuum tube, calculated using Equations (1) to (7), is given by Equation (15):

$$I = \frac{12 \times 3600}{\pi} \times 1367 \times \left[1 + 0.033 \cos \left(\frac{360^\circ \times 110}{365} \right) \right] \times [\cos \delta (\sin \omega_2 - \sin \omega_1)] + \quad (15)$$

$$\frac{2\pi(\omega_2 - \omega_1)}{360^\circ} \sin \phi \sin \delta = \frac{12 \times 3600}{\pi} \times 1367 \times [1 + (0.033 \times (-0.317))] \times [0.866 \times 0.9809 \times 0.966] + 1.0472 \times \frac{1}{2} \times 0.1947 = 152.6 \text{ W/m}^2$$

The thermal conversion efficiency of the vacuum tube collector is expressed as:

$$\eta_Z = \frac{395.76 \times 10^3}{1.8 \times 47 \times 10^{-3} \times I \times 12 \times 3600} \approx 0.7096 \quad (16)$$

For the cooled PV/T system, the heat extracted from the PV module backplate is calculated as follows: during the morning and noon periods, 3000 mL and 3200 mL of water were circulated, respectively, with average temperatures of 25.59°C and 37.77°C. In the afternoon, 2100 mL of water was circulated at an average temperature of 35.25°C. Assuming the working medium (water) has a density of $\rho = 1.0 \times 10^3 \text{ kg/m}^3$, the heat extracted is calculated using Equation (14), as shown in Equation (17):

$$Q_2 = 4.2 \times 10^3 \times \left[\frac{3200 + 3200 + 2100}{10^6} \times 1.0 \times 10^3 \right] \times (36.49 - 25.14) = 395.66 \text{ kJ} \quad (17)$$

4.2.2. Electrical performance of the model

The energy-receiving area of the PV modules in the PV/T system is calculated using Equation (8):

$$A = 63 \times 10^{-2} \times 47.5 \times 10^{-2} \approx 0.2993 \text{ m}^2 \quad (18)$$

Using Equation (9), the fill factor was calculated for both the case without an aluminum foil heat collection plate and copper circulation channel, and the case with circulation. Standard testing with a simulated light source revealed that the maximum power of the PV modules used in the experiment was 37.764 W, with a short-circuit current of 2.31 A. The fill factor for the PV modules in this experiment was calculated to be 0.71.

Using Equation (10), the conversion efficiency was calculated for both the control group PV modules and the cooled PV modules with water circulation. The conversion efficiencies for the control group were 12.87% in the morning, 12.08% at noon, and 8.2% in the afternoon. For the cooled PV modules, the conversion efficiencies were 12.86% in the morning, 12.04% at noon, and 14.03% in the afternoon. Thus, the conversion efficiency of the

cooled PV/T system improved by approximately 1.92%.

The electrical output of the PV modules was calculated using Equation (11). Based on monitoring data, the total solar irradiance on April 20 was 24.81 MJ/m², resulting in a power generation of 0.68 kW·h for the PV modules.

4.2.3. Overall energy efficiency of the model

The solar radiation during the noon period is calculated using Equation (12):

$$Q_Z = (0.2993 + 1.8 \times 47 \times 10^{-3} \times 3) \times 902.52 \times 43200 = 21564740.68W \cdot S \quad (19)$$

After unit conversion, $Q_Z = 21.56$ MJ, the energy absorbed by the PV modules is given by:

$$Q_g = 0.68 \times 3.6 = 2.45MJ \quad (20)$$

In the entire PV/T system, the energy used by the PV modules for power generation is approximately 0.32 MJ, with dissipated energy of about 2.13 MJ. Using Equation (18) and the dissipated energy of 2.13 MJ, the utilization rate of the PV backplate residual heat is calculated to be 18.78%.

The overall energy efficiency of the system is derived using Equations (13), (17), and (19):

$$\eta_Z = \frac{(70.96\% \times 9.9) + (0.32 + 0.4)}{21.56} = \frac{7.75}{21.56} = 0.3595 \quad (21)$$

5. Conclusion

This study primarily employs a comparative research method to investigate the impact of temperature on the output performance of solar photovoltaic (PV) modules. Based on the designed cooled PV/T system, experimental data collection combined with theoretical derivations was used to analyze the system's output performance, including electrical performance, thermal performance, and energy utilization efficiency. The results demonstrate that the designed solar cooled PV/T system exhibits excellent output performance, with a backplate residual heat utilization rate of 18.58% and an overall power generation efficiency improvement of 1.92%. Additionally, due to its small footprint, the system can be extended to ordinary rural areas for heat collection and can meet the electricity demands of low-power electrical devices.

Disclosure statement

The authors declare no conflict of interest.

References

- [1] Yan X, 2022, Discussion on Educational Issues for New Energy Professionals. *Acta Energetica Solaris Sinica*, 43(03): 507–508.
- [2] Wang K, Zhao Y, Zhang Q, et al., 2015, Discussion on New Advances in Comprehensive Utilization of PV/T Collectors. *Technology Innovation and Application*, (3): 1–5.
- [3] He Y, Dai Y, 2020, Experimental Study on a Solar Heat Pump Water Heating System Based on PV/T. *Acta Energetica Solaris Sinica*, 41(12): 83–89.

- [4] He Y, Xiao L, Feng M, et al., 2016, Design Method and Application Study of Photovoltaic/Thermal (PV/T) Solar Systems Based on Model Analysis. *Acta Energetica Sinica*, 37(11): 2937–2944.
- [5] Xu S, 2023, Performance Analysis of Rooftop Solar PV/T Systems. *China Plant Engineering*, (02): 118–121.
- [6] Shmelev AN, Geraskin NI, Apse VA, et al., 2023, Evaluating Conditions and Possibilities for Neutron Catalysis of Thermonuclear Reactions in Three-Component (D-T3-He)-Plasma. *Physics of Atomic Nuclei*, 85(9): 1491–1496.
- [7] Du T, Ma J, Chen X, et al., 2023, Comparative Testing and Numerical Simulation Analysis of Composite Cooling Modes for PV/T Modules. *Chemical Industry and Engineering Progress*, 42(02): 722–730.
- [8] Dong D, Qin H, Liu C, et al., 2013, Research Progress on Solar Photovoltaic/Thermal (PV/T) Technology. *Chemical Industry and Engineering Progress*, 32(05): 1020–1024.
- [9] Razali N, Fudholi A, Ruslan M, et al., 2019, Experimental Study of Water-Based Photovoltaic Thermal (PVT) Collector. *International Journal of Electrical and Computer Engineering*, 9(1): 118–125.
- [10] Khanjari Y, Pourfayaz F, Kasaeian A, 2016, Numerical Investigation on Using Nanofluid in a Water-Cooled Photovoltaic Thermal System. *Energy Conversion & Management*, 122: 263–278.
- [11] Nasrin R, Rahim N, Fayaz H, et al., 2018, Water MWCNT Nanofluid-Based Cooling System of PVT: Experimental and Numerical Research. *Renewable Energy*, 121: 286–300.
- [12] Liu S, Feng H, 2012, Impact of Randomness on Photoelectric Conversion Efficiency in Photovoltaic Power Generation. *Journal of Chifeng University (Natural Science Edition)*, 28(23): 5–7.
- [13] Guo G, Gou Y, Zhong X, 2022, Simulation Study on the Impact of Different Cross-Sectional Flow Channels on PV/T System Performance. *Integrated Intelligent Energy*, 44(4): 76–84.
- [14] Zhang H, 1990, Principles of Solar Thermal Utilization and Computer Simulation. Northwestern Polytechnical University Press, 1990: 10–43.
- [15] He D, He T, Ding H, 2012, Principles and Application Technologies of Solar Photovoltaic Power Generation Systems. Chemical Industry Press, 2012: 41–42.

Publisher's note

Bio-Byword Scientific Publishing remains neutral with regard to jurisdictional claims in published maps and institutional affiliations.